DAPNIA/SEA-00-15

TESLA Linear Collider : Status Report

O. Napoly
for the TESLA Collaboration

CEA/Saclay, DAPNIA/SEA
91191 Gif-sur-Yvette, FRANCE

Presented at the Linear Collider Workshop 2000 (LCWS 2000)
October 24-28, 2000, FNAL, Batavia, IL, USA

TESLA Linear Collider : Status Report

O. Napoly
for the TESLA Collaboration

CEA/Saclay, DAPNIA/SEA
91191 Gif-sur-Yvette, FRANCE

Abstract.
We review the current status of the R&D results and design studies on the TESLA superconducting e^+e^- linear collider project.

I OVERVIEW

The feasibility of a linear collider has been demonstrated by the successful operation of the SLAC Linear Collider (SLC). However, aiming at c.m. energies at the TeV scale with luminosities around $10^{34}\mathrm{cm}^{-2}\mathrm{s}^{-1}$, the next generation of linear colliders require at least 100 times higher *beam powers* and 100 times smaller *beam sizes* at the collision point.

The fundamental difference of the TESLA approach compared to other designs is the choice of superconducting accelerating structures. TESLA uses 9-cell Niobium cavities (figure 1) cooled by superfluid Helium to $T = 2\,\mathrm{K}$ and operating at 1.3 GHz RF frequency. The design gradient at $E_{cm} = 500\,\mathrm{GeV}$ is $E_{acc} = 23.4\,\mathrm{MV/m}$. Because the power dissipation in the cavity walls is extremely small, the accelerating field can be produced with long, low peak power RF-pulses. This results in a high RF to beam power transfer efficiency, allowing a high average *beam power* while keeping the electrical power consumption within acceptable limits ($\sim$100 MW). Secondly, extremely small *beam sizes* at the interaction point (IP) require preserving ultra-small emittance beams in the linac. This is well suited with the relatively low frequency (large dimensions) of the TESLA cavities and their accordingly weak wakefields (beam-cavity interaction).

The choice of superconducting RF also allows one to use a long RF-pulse (1 ms) and a relatively large bunch spacing (337 ns at $E_{cm} = 250\,\mathrm{GeV}$). Three benefits result directly from this long bunch train:

- A fast (MHz) bunch-to-bunch feedback can be used to correct the orbit within one beam pulse. Such a feedback system will maintain the beams in collision at the IP, making TESLA relatively insensitive to mechanical vibrations which could otherwise lead to serious luminosity reduction.

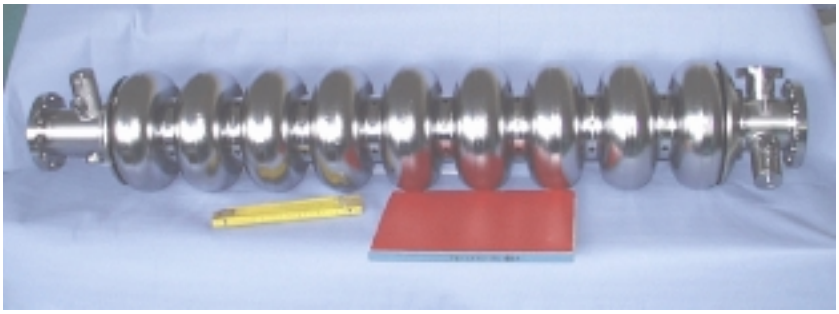

FIGURE 1. The 9-cell Niobium cavity for TESLA.

- In the event of an emergency, a fast safety system can "turn off" the beam within a fraction of a pulse.
- Each bunch collision can be tagged by the detector and the detector background isolated.

Making use of these unique features has led to a parameter set (see table 1) which clearly demonstrates TESLA's potential for high luminosity. In comparison with the earlier design [1], about a factor of five improvement in the luminosity is achieved, while maintaining a low level of beamstrahlung.

Upgrading the collider up 800 GeV cm energy on the same site requires increasing the accelerating gradient up to 35 MV/m, well below the 50 MV/m fundamental limit for Niobium structures at 2 K, together with a slightly closer packing of the RF cavities as provided by the susperstruture concept (see Sect.2). A higher luminosity can only be obtained by raising the beam and RF powers : it therefore requires doubling the number of klystrons and approximately doubling the cooling capacity the cryogenic plants.

II STATUS OF R&D ON SC RF CAVITIES

In order to demonstrate the feasibility of the high-gradient cavity technology and to create a solid basis for a reliable cost estimate of future large-scale production, the TESLA collaboration is running an R&D program centered around the TESLA Test Facility (TTF) [2]. The TTF includes the infrastructure for applying different processing techniques to the Niobium cavities obtained from industrial production and a 120 m long linac designed, built and commissioned by the members of the TESLA collaboration. The schematic layoyt of the linac is shown in Fig.2.

As shown by Figs.3,4, gradients in excess of 25 MV/m are regularly obtained in large series of industrially produced TESLA cavities. In the third cryomodule installed in the TTF linac, the maximum usable gradient was determined for each of the eight cavities : the average gradient was 23.6 MV/m, indicating that installation of the individual cavities into a module does not degrade their performance. The

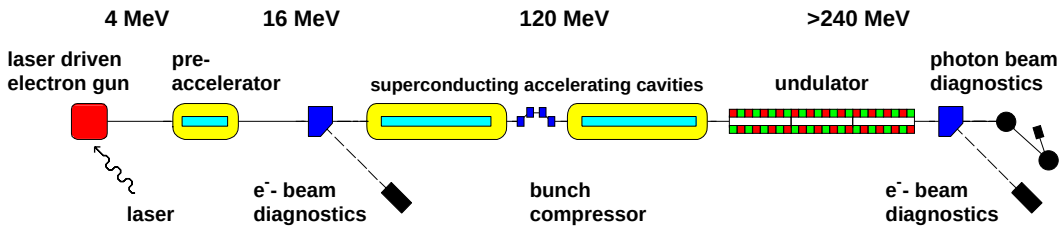

FIGURE 2. Schematic layout of the TESLA Test Facility Linac (TTFL).

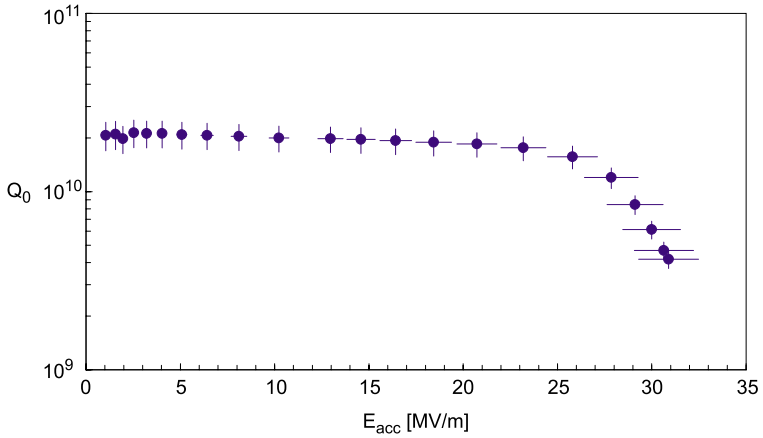

FIGURE 3. Excitation curve of a high-performance TESLA 9-cell cavity. The cavity was cooled by superfluid helium of 2 K. The systematic rms errors in the determination of the accelerating field and the quality factor Q_0 are indicated.

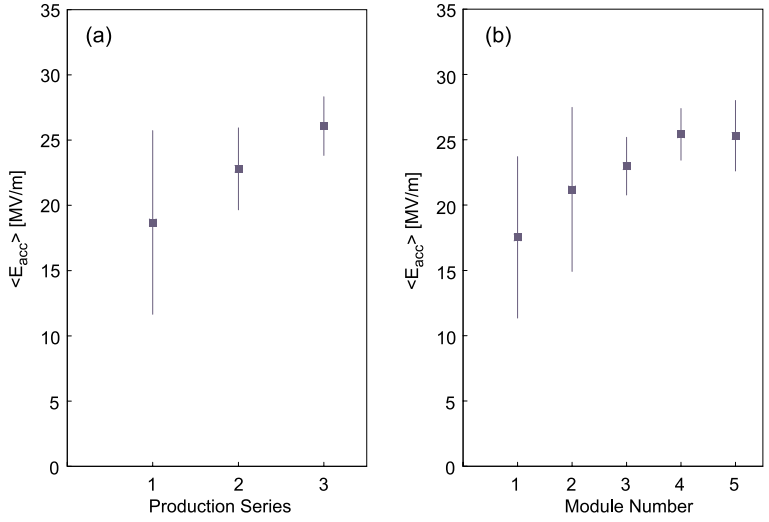

FIGURE 4. Average accelerating gradients at $Q_0 \geq 10^{10}$ measured in the vertical test cryostat of: (a) the cavities in the three production series; and (b) the cavities installed in the first five cryogenic modules for TTF.

energy upgrade to 800 GeV uses of the so-called 'superstructure', where the effective acceleration length is increased by combining two multicell cavities (see Fig.5) with a reduced inter-cavity spacing $\lambda_{RF}/2$ and, the number of RF-input couplers is halved by powering them with a single high power coupler. The accelerating field gradient required is then 35 MV/m which, although already approached by a few exceptional TTF cavities, represents a significant increase compared to the performance achieved so far. Such high gradients have been reached in a reproducible manner in single-cell cavities, as shown by Fig.6, by applying a new cavity preparation procedure investigated jointly by KEK, CERN, DESY and Saclay. It involves 'electropolishing' by which the RF surface material is removed in an acid mixture under current flow, followed by clean water rinsing and baking at moderate temperature (100-150°C). This new method might allow to omit the time-consuming 1400°C heat treatment which prevails in the current production.

Accelerating gradient	E_{acc} [MV/m]	23.4
RF-frequency	f_{RF} [GHz]	1.3
Fill factor		0.747
Total site length	L_{tot} [km]	33
Active length	[km]	21.8
# of acc. structures		21024
# of klystrons		584
Klystron peak power	[MW]	9.5
Repetition rate	f_{rep} [Hz]	5
Beam pulse length	T_P [μs]	950
RF-pulse length	T_{RF} [μs]	1370
# of bunches p. pulse	n_b	2820
Bunch spacing	Δt_b [ns]	337
Charge p. bunch	N_e [10^{10}]	2
Emittance at IP	$\gamma\epsilon_{x,y}$ [10^{-6}m]	10, 0.03
Beta at IP	$\beta^*_{x,y}$ [mm]	15, 0.4
Beam size at IP	$\sigma^*_{x,y}$ [nm]	553, 5
Bunch length at IP	σ_z [mm]	0.3
Beamstrahlung	δ_E [%]	3.2
Luminosity	L_{e+e-} [10^{34}cm^{-2}s^{-1}]	3.4
Power per beam	P_b [MW]	11.3
Two-linac primary electric power	P_{AC} [MW]	105
e^-e^- collision mode:		
Beamstrahlung	$\delta_{E,e-e-}$ [%]	2.0
Luminosity	L_{e-e-} [10^{34}cm^{-2}s^{-1}]	0.47
$\gamma\gamma$ collision mode:		
Emittance at IP	$\gamma\epsilon_{x,y}$ [10^{-6}m]	3, 0.03
Beam size at IP	$\sigma^*_{x,y}$ [nm]	157, 5
Geometric luminosity	L_{geom} [10^{34}cm^{-2}s^{-1}]	5.8
Effective $\gamma\gamma$ luminosity	$L_{\gamma\gamma}$ [10^{34}cm^{-2}s^{-1}]	0.6

TABLE 1. TESLA parameters for the $E_{cm} = 500$ GeV baseline design, the e^-e^- and $\gamma\gamma$ modes of operation.

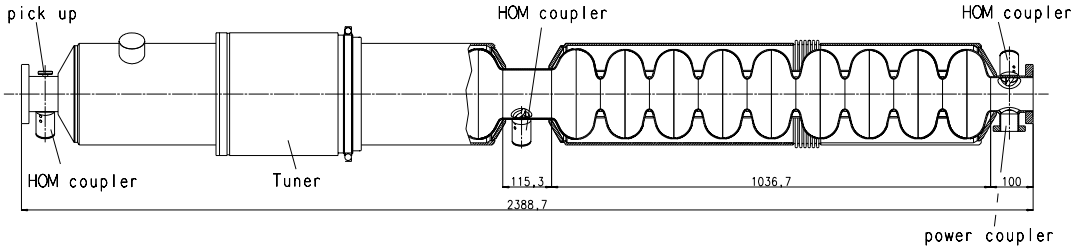

FIGURE 5. Superstructure II consisting of two 9-cell resonators joined by a 114 mm beam pipe. The power coupler is at one end.

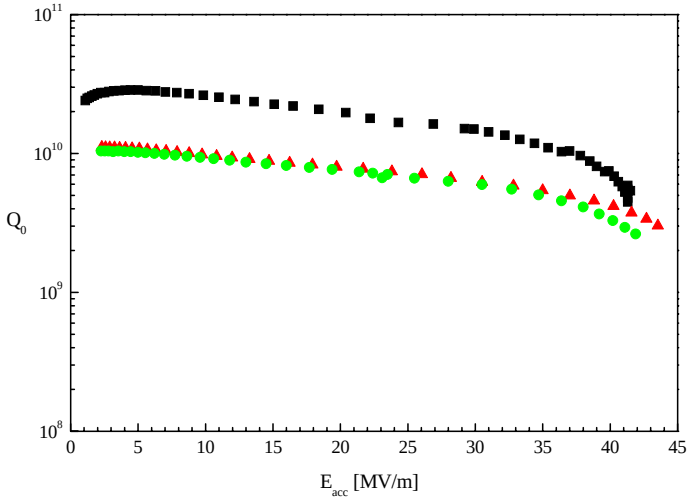

FIGURE 6. Excitation curves of three electropolished single-cell cavities without heat treatment at 1400°C.

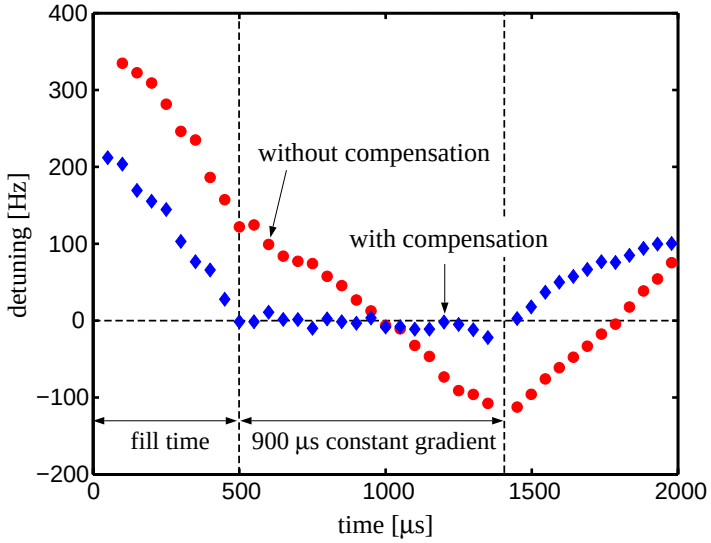

FIGURE 7. Piezoelectric compensation of the Lorentz-force induced frequency shift pulsed-mode cavity operation. The accelerating field is 23.5 MV/m.

The RF detuning of the cavity induced by its mechanical deformation due to the internal electromagnetic radiation pressure, has been identified as an outstanding problem beyond 25 MV/m gradient. Below this gradient the current mechanical stiffening of the multicell cavity is sufficient. To allow for higher gradients the stiffening must be improved, or alternatively, the cavity deformation must be compensated. The latter approach has been successfully demonstrated using a piezoelectric tuner (see Fig.7). The result indicates that the present stiffening augmented by a piezoelectric tuning system will permit efficient cavity operation at the TESLA-800 gradient of 35 MV/m.

III COLLIDER DESIGN

The TESLA collider layout is shown in Fig.8. It includes an X-ray free electron laser user facility which will exploit the first 50 GeV section of the electron linac. We discuss here only the e^+e^- collider main sub-systems, starting with the e^+ and e^- sources.

A Injection System and Damping Rings

The electron beam is generated in a polarized laser-driven gun based on the GaAs photocathode technology developed for the SLC, [3] where the electron polarization reached 80%.

The positron injection system has to provide a total charge of about $5.6 \cdot 10^{13} e^+$ per beam pulse, which is not feasible with a conventional (electron on thick target) source. Instead, positrons are produced from γ-conversion in a thin target (see Fig.9). The photons are generated by passing the high-energy electron beam through an undulator placed after the main linac, before transporting the beam to the IP. Passage through the undulator causes the energy spread in the electron beam to increase from $0.5 \cdot 10^{-3}$ to $1.4 \cdot 10^{-3}$, with an average energy loss of 1.2 %, both of which appear tolerable. Besides providing a sufficiently high positron beam intensity, the undulator-based source offers several advantages: a) use of a thin target leads to a smaller positron beam with a smaller transverse emittance than from a conventional (thick target) source; b) *polarized* positrons is possible by replacing the planar undulator with a helical undulator. The polarised positron option is technically more ambitious and is considered a potential upgrade at a later stage of operation. The achievable polarisation ranges from 45% to 60%. The undulator-based method requires an electron beam energy of at least 150 GeV for full design positron beam intensity. Therefore at center-of-mass energies below 300 GeV the luminosity is reduced due to a lower positron beam current. Running on the Z_0 peak can be done by by-passing the 46 GeV electron beam to the IP, while using the remaining 200 GV electron acceleration to drive the positron source.

Both beams are injected into damping ring at 5 GeV energy. The bunch train is stored in the ring in a compressed mode, with the bunch spacing reduced by about

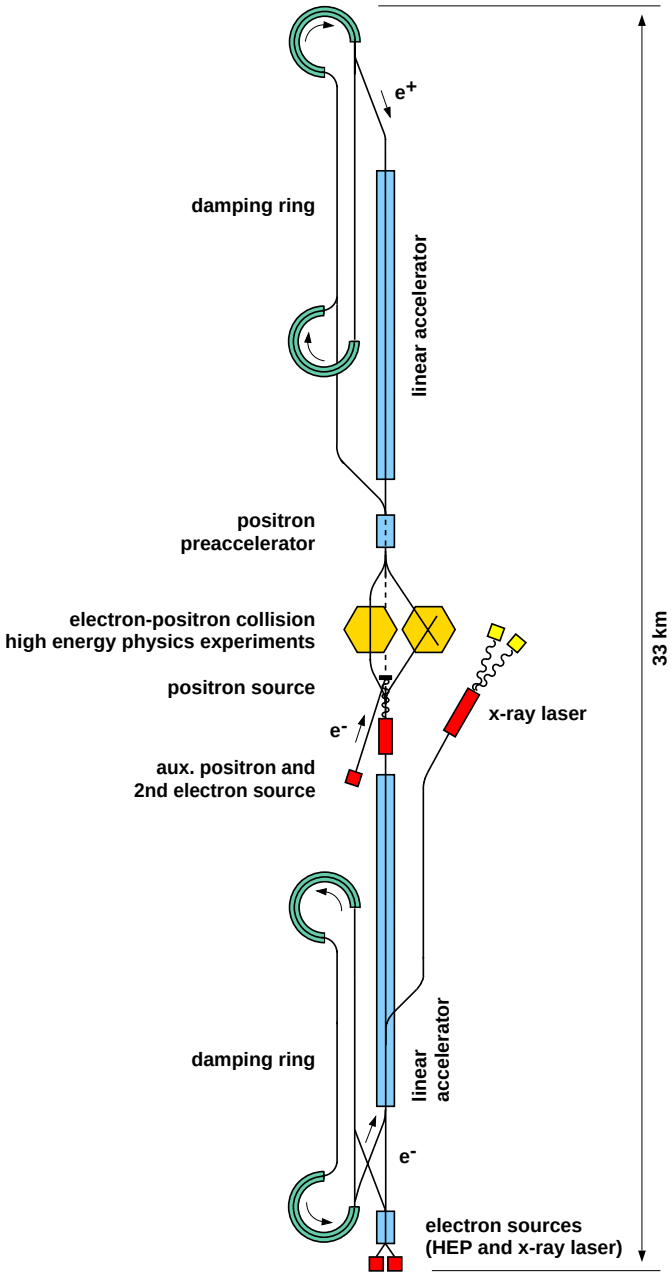

FIGURE 8. Sketch of the overall layout of TESLA.

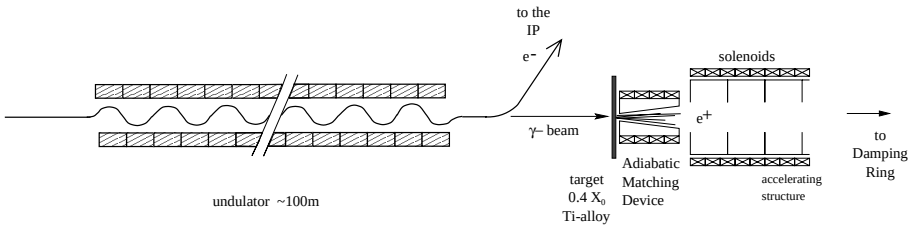

FIGURE 9. Sketch of the positron source layout.

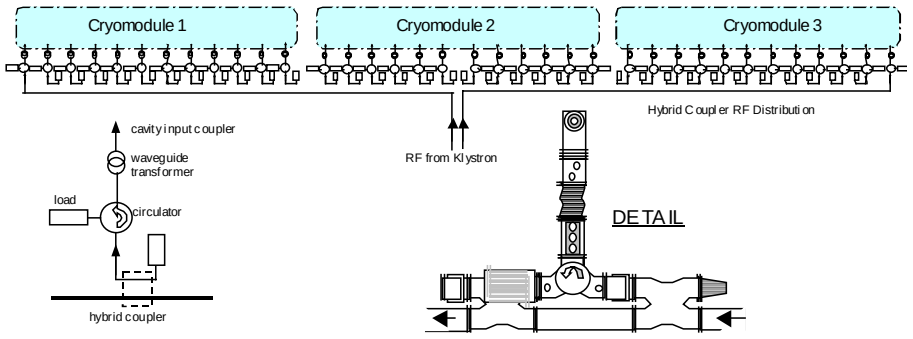

FIGURE 10. RF waveguide distribution of one RF station

a factor of 16; even with this compression, a large ring circumference of about 18 km is still needed. To avoid building an additional large ring tunnel, a so-called "dog bone" design is used (see Fig.8). The damping ring optics is designed to achieve $8 \cdot 10^{-6}$ m horizontal and $0.02 \cdot 10^{-6}$ m vertical emittances (normalized), providing a 50% margin for vertical emittance degradation until the IP. About 400 m of wiggler section are needed to achieve sufficient damping time (28 ns). Fast kickers are required for compression and decompression of the bunch train at injection and extraction respectively.

Despite its unconventional shape, the damping ring does not exhibit any unusual beam dynamics. The only exception, related to the large ratio of circumference to beam energy, is a large incoherent space charge tune shift. The effect can be significantly reduced, however, by raising the beam energy and artificially increasing the beam cross-section in the long straight sections which dominates the space charge effect. To do so, the beam is transversely fully coupled in the straight sections by inserting skew sextupoles.

B Main Linac

The two main linear accelerators are each constructed from roughly ten-thousand one-meter long superconducting cavities. Groups of twelve cavities are installed in a common cryostat (cryomodule) whose design is based on that successfully used in the TTF, modified to be more modular and cost-effective. As shown by Fig.10,

FIGURE 11. The Thomson TH1801 multibeam klystron.

groups of 3 cryomodules, or 36 cavities, are powered by a single 10 MW multibeam klystron with two RF output windows. Such a klystron, with seven beams, has been tested (see Fig.11) at 10 MW with an efficiency close to the 70% design one. In the baseline design, the coaxial coupler must transmit about 230 kW (24 MV $\times$ 9.5 mA) peak RF power, well below the 1.6 MW achieved by TTF couplers.

The cryogenic system for the TESLA linac is comparable in size and complexity to the one currently under construction for the LHC at CERN.

Beam dynamics studies have been undertaken to specify the linac tolerances on the cavity and quadrupole alignment and, on the damping of long range wakefields. The realistic alignment errors after installation and survey of the linac modules are 0.5 mm (rms) for the cavities and 0.3 mm (rms) for the quadrupoles. As shown by Fig.12, the single bunch emittance growth resulting from short range wakefields excited in misaligned cavities is about 7%, with an additional 6% for a one σ_y injection error. The dispersive effect of quadrupole misalignments can be much larger unless it is compensated by beam-based alignment methods. Relying on a BPM resolution of 10 μm (rms), beam-based correction algorithms aleady used at the SLC limit the dispersive emittance growth to a few %. These effects are well contained within the 50% margin in vertical emittance coming from the damping rings.

With a train of bunches, the long-range wakefields excited by each bunch will act on the subsequent bunches, resulting in a possible multi-bunch emittance growth. In order to reduce the effective wake along the TESLA bunch train, a small damping of the higher order modes (HOM) is required. The lifetime of the modes is reduced by means of HOM dampers, which are mounted at both ends of a TESLA cavity. The multi-bunch transverse profile resulting from a given set of cavity alignment

errors is shown in Fig.13. It is significant only in the head of the bunch train and the emittance growth integrated over the complete bunch train is negligible. Moerevoer, its pattern is stable with time which opens the possibility to remove most of it by a fast intra-pulse orbit correction system.

C Beam Delivery System

The complete beam delivery system (BDS) layout (linac to linac) is shown in Fig.14, including the optional second IP. It consists of beam switch-yard, collimation, beam diagnostics and correction and final focus sections. By putting the undulator based e^+ source in front of the electron beam switch-yard, both IP's can host e^+e^- collisions, while $\gamma\gamma$ collisions which require a non zero crossing angle can take place only at the second IP. The primary e^+e^- BDS and interaction region are described in more detailed elsewhere in these proceedings [4]. The main extraction beam line transport the spent beams almost loss-free to the dump halls, on both sides of the IP. An fast emergency extraction line, starting in front of the collimation section, brings the beams to the main dump system. It is primarily intended to extract some fraction of the bunch train in the event of a machine protection trip. It will also serve as a by-pass line during commissioning.

Due to the high vertical disruption parameter at the IP ($D_y \approx 25$), the luminosity is extremely sensitive to small offsets in both beam-beam displacement and crossing angle. As a result, the collisions must be maintained to within $\sim 0.1\sigma$ in both offset and angle, or 0.5 nm and 1.2 μrad respectively. Figure 15 illustrates the concept for the IP beam separation feedback system. The large TESLA bunch spacing of

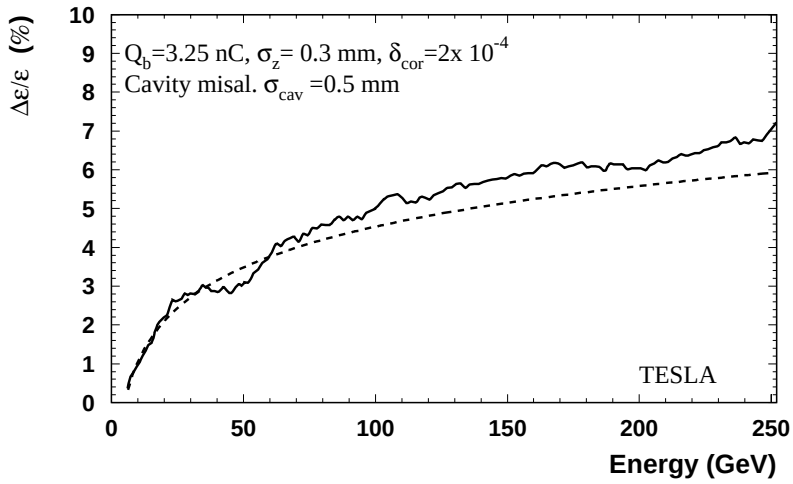

FIGURE 12. Vertical emittance growth obtained from simulation of 50 random cavity misalignments (δy_c=0.5 mm rms). The dashed curve is the analytical prediction from a two-particle model.

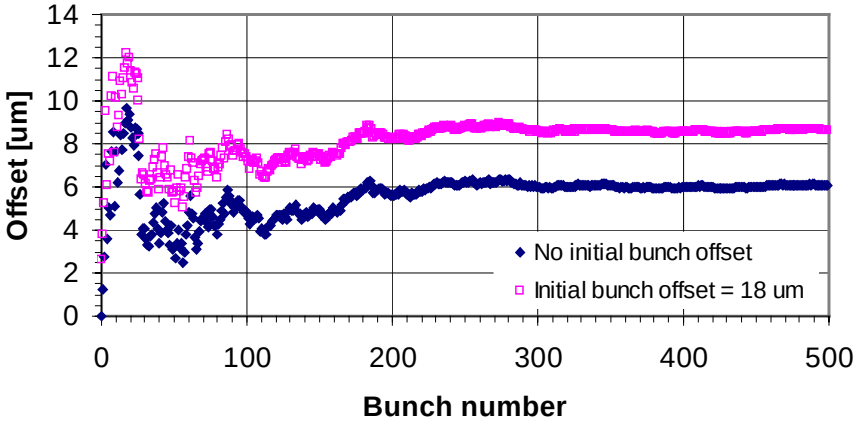

FIGURE 13. Orbit offsets in μm of the first 500 bunches at the end of the linac. The lower curve shows the effects of cavity misalignments only ($\Delta y_c = 0.5\,\mathrm{mm}$ rms, one seed). The upper curve shows the effects of the same misalignments, but with a one $1 \times \sigma_y$ injection error of the beam.

337 ns allows the use of a digital controller. Fast kickers ($\sim$100 ns) are used to make the necessary orbit corrections. The feedback signal is derived directly from the strong beam-beam kick which both beams experience when they do not collide head-on. Such a feedback system, successfully used at the SLC [5], can correct up to 200 nm motion of the last doublet at frequencies $f \ll 3\,\mathrm{MHz}$ with a luminosity loss smaller than 10%. The implementation of the high resolution BPM's (5 μm on a bunch to bunch basis) within the final doublet and IP region is shown in Fig.16. The tungsten mask shown in this figure shields the detector from the copious e^+e^- pair background produced in the beam-beam interaction. It also supports a fast luminosity monitor using the incoherent e^+e^- pair signal. This detector, able to accurately measure luminosity variations on a bunch to bunch basis, provides a powerful mean to optimize the collider and could be included in the fast feedback algorithm.

IV CONCLUSION

Convinced by the reliability and the potential of the TESLA technology, the TESLA collaboration will release a Technical Design Report (TDR) in March 2001. This report will include a cost estimate for the collider, with an additional cost for the XFEL facility, as well as an implementation study on the DESY site. The construction time, including tunneling, cryomodule production and installation is foreseen to be 8 years. The TDR will also start the process of project evaluation at a national (submission to the German Science Council in 2001) and international level before an international collaboration can be formed.

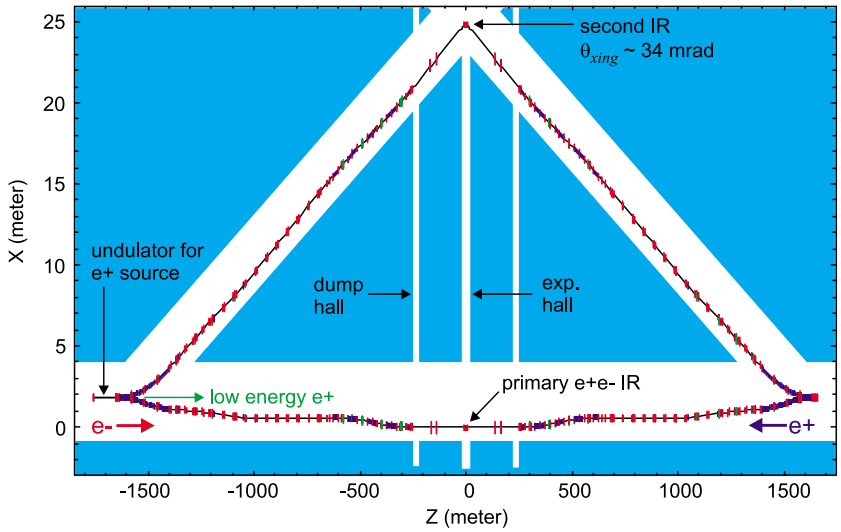

FIGURE 14. Geometry of the TESLA BDS, including the second IR.

REFERENCES

1. R. Brinkmann, G. Materlik, J. Roßbach and A. Wagner (eds.), *Conceptual Design of a 500 GeV e+e- Linear Collider with Integrated X-ray Laser Facility*,
2. *Proposal for a TESLA Test Facility*, DESY-TESLA-93-01, 1992.
3. R. Alley, et.al., *The Stanford Linear Accelerator Polarised Electron Source*, Nucl. Inst. and Meth. **A 365**, p.1, 1995.
4. O. Napoly and N. Walker, *TESLA IR Layout, Collimation and Extraction*, these proceedings.
5. F. Rouse, T. Gromme, W. Kozanecki, N. Phinney, *Maintaining Micron Size Beams in Collision at the Interaction Point of the Stanford Linear Collider*, SLAC-PUB-5512 (1991)

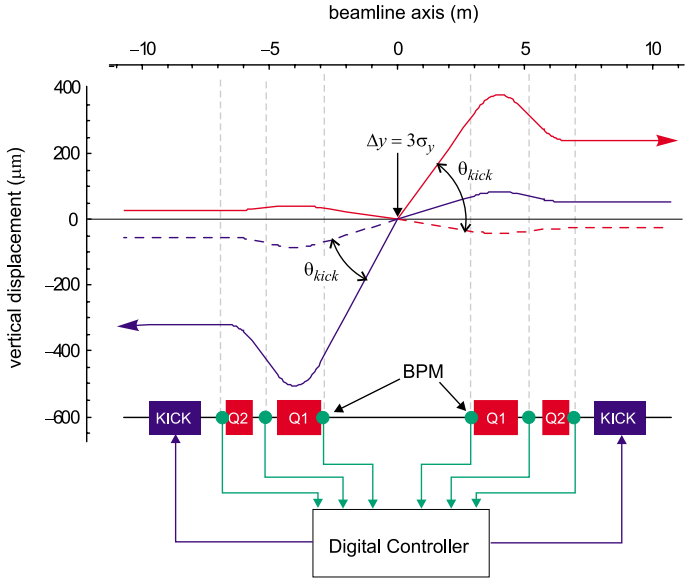

FIGURE 15. The IP fast feedback system. The red and blue rays represent an example having a $3\sigma_y^*$ offset at the IP (corresponding approximately to a $10\sigma_{y'}^*$ kick). The dotted lines represent the trajectories with no beam-beam kick.

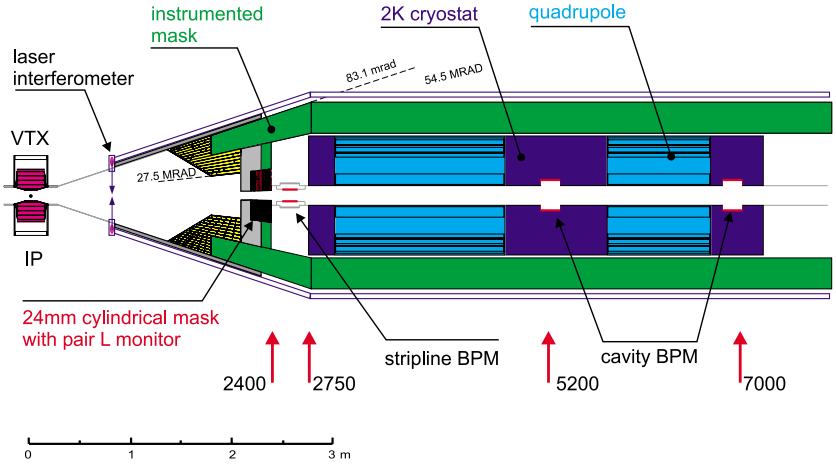

FIGURE 16. Interaction region layout.